Effects of debinding condition on thermal conductivity of pressureless sintered AlN

Seung-Il Kim[a], Shin-Il Go[a], Seong-Ro Lee[b] and Sang-Jin Lee[c],*

[a]*Research & Development Lab., YJC Co., Hyampyung, 525-813, Korea*
[b]*Department of Information Electronics Engineering, Mokpo National University, Muan, 534-729, Korea*
[c]*Department of Advanced Materials Science and Engineering, Mokpo National University, Muan, 534-729, Korea*

The effects of debinding condition on the thermal conductivity of AlN pressureless sintered at 1850 °C for 5 h in a N_2 atmosphere were investigated. Spray dried AlN powder compacts incorporating 3 ~ 5 wt% Y_2O_3 sintering additive and 0.5 wt% PVB binder were calcined in air or a N_2 atmosphere for binder burn-out. The debinding condition affected the second phase, the second phase distribution, and the thermal conductivity of the sintered AlN samples. All sintered AlN samples were densified to higher than 98% theoretical density. The sample debinded in a N_2 atmosphere showed higher thermal conductivity (170 W/mk) than that of the sample debinded in an air atmosphere (< 140 W/mk). In the sample debinded in the air atmosphere, a YAG phase, $Y_3Al_5O_{12}$, was observed as the secondary, intergranular phase showing a wide distribution. On the other hand, when the debinding process was conducted in a N_2 atmosphere, $Y_4Al_2O_9$, $YAlO_3$ and Y_2O_3 phases were observed at the triple point, and the sample color was different at the sample surface and interior due to the residual carbon. In this study, a commercial, spray dried AlN powder was also sintered and examined to confirm the obtained results.

Key words: AlN, Debinding, Thermal conductivity, YAG, Firing atmosphere.

Introduction

Sintered aluminum nitride (AlN) has been recognized as an attractive material in recent years because it has high thermal conductivity (a single crystal has thermal conductivity of about 320 W/mk), a low dielectric constant, good electrical insulation, and a low thermal expansion coefficient (4.4×10^{-6}/°C). However, the thermal conductivity of dense polycrystalline AlN is significantly reduced by impurities, especially by oxygen and carbon [1]. AlN has low diffusivity and requires high sintering temperatures (1800 ~ 2000 °C). Covalent bonding between Al and N makes the sintering of AlN difficult, however, without the application of sintering additives [2, 3]. In general, Y_2O_3 is an especially good sintering additive for liquid phase sintering of AlN. The room temperature thermal conductivity of polycrystalline AlN prepared by liquid-phase sintering, is reported to be 100 ~ 260 W/mK [4]. This significant reduction in thermal conductivity is caused by the presence of oxygen impurities [5]. In the AlN sintering process, Y_2O_3 additive reacts with the surface oxide layer of AlN particles, and forms a liquid phase of a Y-Al-O-N system that promotes particle rearrangement and densification. This causes precipitation of yttrium-aluminum-oxide phases such as YAG, YAM, and YAP in grain boundaries and lowers the oxygen content

dissolved in AlN grains, and the thermal conductivity of sintered AlN thereupon increases [6, 7]. Besides oxygen, carbon is also believed to be an important impurity that affects the thermal conductivity of AlN, although the mechanism is not completely understood. Regarding the sintering behavior of AlN, used as an additive, carbon directly enhances the grain-growth rate of AlN and retards densification. A certain amount of carbon is needed to reduce the oxygen impurity level by carbon de-oxidation, where the free carbon reacts with the oxygen producing carbon monoxide gas [8-10]. The carbon amount as well as sintering aids affects the thermal conductivity of AlN. It was previously reported that residual carbon with Y_2O_3 as a combined sintering aid reduced the oxygen level in AlN powder during the sintering process, reduced the amount of the grain boundary phase, and slowed down the grain growth of AlN [8]. In the sintering process of AlN, granule-type powder is used for convenience of homogeneous mixing of the sintering aid and forming a green body. Normally, AlN powder is granulated with an organic binder in the spray dryer process. To add some carbon to AlN, many types of carbon additives are employed in the preparation process of AlN powder. As another method of carbon addition, the decomposed binder in the spray dried AlN granule can act as a carbon source.

In this study, spray dried powders prepared with phase-free AlN powder were used to examine the effects of the debinding atmosphere on the thermal conductivity of densified AlN. A Y_2O_3 sintering aid and polyvinyl butyral (PVB) binder were added to the

*Corresponding author:
Tel : +82-61-450-2493
Fax: +82-61-450-2498
E-mail: lee@mokpo.ac.kr

granule-type AlN powder. An air or N_2 atmosphere was applied for the debinding process. The binder burn-out behavior and the effect of the residual carbon on the thermal conductivity of AlN were examined. In addition, the results were compared with data obtained from sintered AlN prepared with a commercial spray dried AlN powder.

Experimental Procedure

A phase-free AlN powder (H-grade, Tokuyama Soda, Japan) was used as the starting powder, and Y_2O_3 powder (C-grade, H.C.Strack, Germany) was used as the sintering aid. A commercial spray dried AlN powder (HT-grade, Tokuyama Soda, Japan) was also used for comparison. The mean particle size and purity of the used powders are listed in Table 1. AlN powder (H-Grade) was mixed with 3 wt% or 5 wt% Y_2O_3 powder, respectively, with 0.5 wt% PVB (Butvar, B-98) binder. Mixed powders were ball milled with zirconia ball media (Y-TZP) for 24 h, using an isopropyl alcohol as a mixing solvent. A spray dryer (DJE-FCNM-EP022R, Dongjin Co., Korea) was used for fabrication of the AlN granule powders. The slurry solvent (ethyl alcohol) and the dried powders were mixed to a 1:0.8 wt% ratio. The spray dried powders and commercial powder were uniaxially pressed under 30 MPa pressure with holding time of 5 min. The uniaxially pressed specimens were then cold isostatically pressed under 200 MPa. The

green samples were fired at 600 °C for 6 h in an air atmosphere, or at 600 °C for 6 h in a nitrogen atmosphere, respectively. The debinded specimens were pressureless sintered at 1850°C for 5 h in a N_2 atmosphere. During the sintering, the specimens were embedded with AlN powder. The differences between the specimens with each processing condition are listed in Table 2.

The phase observation of the sintered AlN samples at each debinding condition was conducted using an X-ray diffractometer (Dmax automated powder diffractometer, Rigaku/USA, MA, USA) with CuK_α radiation. The measurements were made with a scanning speed of 10 ° min^{-1} and a sampling interval of 0.02 ° at room temperature. The pyrolysis and decomposition behavior of the PVB binder in air and N_2 atmospheres were monitored by a thermogravimetric analysis (DTA/TGA) (Model STA 409, Netzsch GmbH, Selb, Germany) up to 1000 °C at a heating rate of 10 °C min^{-1}, in an air atmosphere. The microstructural observation of the spray dried powder and sintered AlN was carried out by field emission scanning electron microscopy (FE-SEM, Hitachi, S-4800, Hitachi, Japan) to study the powder morphology and the secondary phase distribution in sintered AlN. The thermal conductivity of the sintered AlN samples was measured by the laser flash technique (KS L 1604:2007) using a thermal diffusivity measurement facility (LFA-447, Netzsch, Germany). The densities of all samples were measured by the Archimedes displacement method.

Results and Discussion

Fig. 1 presents the spray dried AlN powders. The granule-type powders showed a spherical morphology with a size range of 40 ~ 100 μm. The spray powders had excellent fluidity, providing convenience in the pressing forming process.

Fig. 2 shows the DTA/TG curves of the PVB fired up to 1000 °C in an air atmosphere and a N_2 atmosphere for examination of the burn-out behavior. In the TG curve obtained from the air atmosphere, the mass loss occurred in two stages (1) 350 °C to 400 °C and (2)
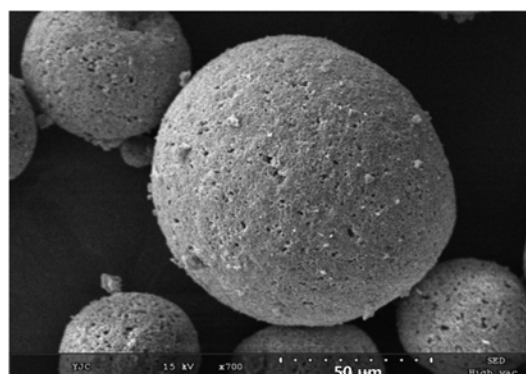
Table 1. Mean particle size and purity of AlN and Y_2O_3 powders.

Powder	Mean particle size (μm)	Chemical impurities [¥]
AlN powder (H-grade)	1.13	O : 0.83 wt% C : 210 ppm
AlN granule (HT-grade)	75	O : 0.83 wt% C : ≅ 0.5 wt%
Y_2O_3 (C-grade)	0.8	99.99%

[¥] Other impurities : Ca, Si and Fe in ppm scale.

Table 2. Differences between specimens with each processing condition.

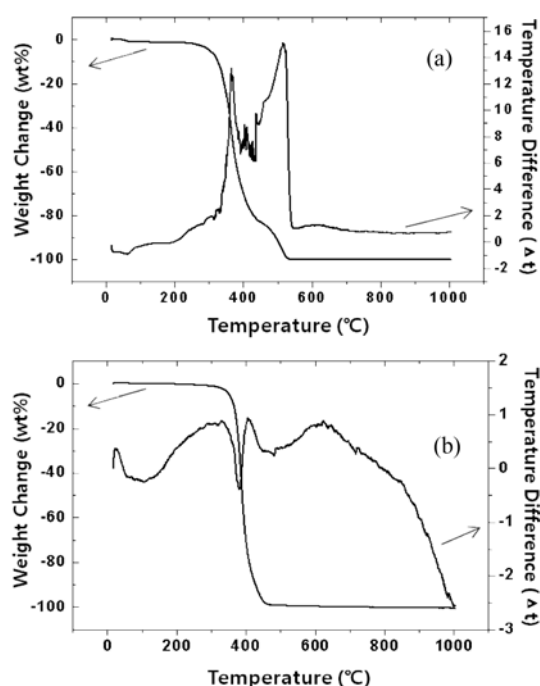| Sample No.	Sintering condition	Material	Debinding condition
#1		AlN, Y_2O_3 (3 wt%), Binder (0.5 wt%)	Air 600 °C / 6 h
#2	1850 °C / 5 h / N_2	AlN, Y_2O_3 (5 wt%), Binder (0.5 wt%)	
#3		Tokuyama Soda 社 , HT-grade	
#4		AlN, Y_2O_3 (5 wt%), Binder (0.5 wt%)	N_2 600 °C / 6 h
#5		Tokuyama Soda 社 , HT-grade	

Fig. 1. Spray dried AlN granules.

Fig. 2. DTA and TG curves of PVB fired at (a) air atmosphere and (b) N_2 atmosphere.
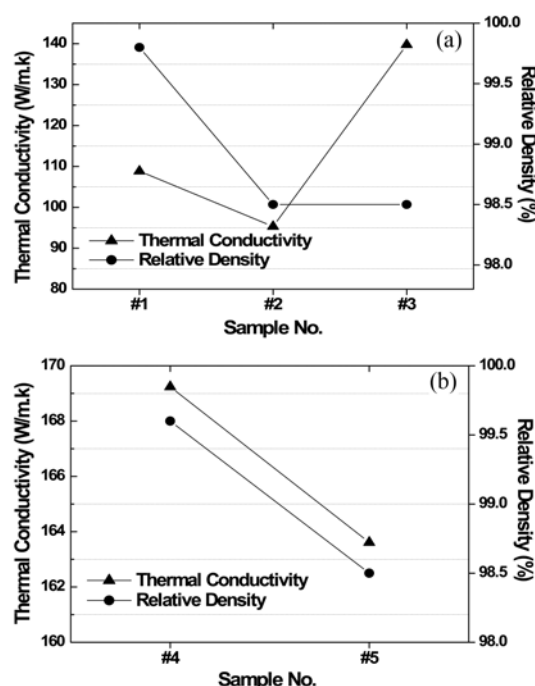

Fig. 3. Relative density and thermal conductivity of sintered AlN samples prepared from different debinding condition of (a) air and (b) N_2 atmosphere.

$400\ ^{\circ}C$ to $500\ ^{\circ}C$. The DTA spectrum showed two exothermic peaks at the two weight loss ranges. In general, polymer decomposition in an air atmosphere occurs through two steps [9]. The first step is degradation of the polymeric structure by pyrolysis, which is then followed by oxidation of carbons from the decomposed polymer. In the PVB polymer, the first mass loss is
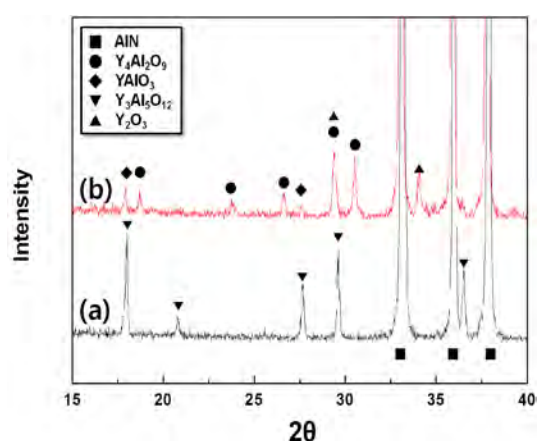

Fig. 4. XRD patterns of AlN samples containing 5 wt% Y_2O_3 sintered at $1850\ ^{\circ}C$ for 5 h after debinding in different condition ; (a) air atmosphere, sample #2 and (b) N_2 atmosphere, sample #4.

thought to be caused by pyrolysis of PVB, which results in breaking of the carbon backbone. The larger exothermic peak in the second weight loss may be due to burn-out of the residual carbons to CO, and CO_2 gases form by an oxidation reaction. In the N_2 atmosphere, significant weight loss was observed at $400\ ^{\circ}C$. At this temperature, most free organics and carbons were removed through thermal decomposition and an exothermic peak was observed at the decomposition range. However, large exothermic peak as detected for oxidation reaction in air atmosphere was not observed. This indicates that residual carbon may remain through the thermal decomposition process in the N_2 atmosphere.

The densified AlN samples showed different sintered density and thermal conductivity. Fig. 3 represents the relative densities and thermal conductivities of the sintered specimens prepared under different debinding conditions. All sintered specimens were densified to higher than 98% theoretical density. In the thermal conductivity examination, the specimens debinded in the N_2 atmosphere showed higher values (> 160 W/mk) than those of the specimens debinded in the air atmosphere (< 140 W/mk). The highest thermal conductivity (about 170 W/mk) was obtained from AlN debinded in the N_2 atmosphere, with the use of 5 wt% Y_2O_3.

Fig. 4 shows the XRD patterns of the AlN specimens sintered after debinding in air and N_2 atmospheres. In the sintered AlN sample debinded in air, a secondary phase, $Y_3Al_5O_{12}$, was observed with the main AlN phase. Normally, YAG, YAM and YAP phases are detected in sintered AlN containing Y_2O_3 additive [11-13]. The formation of the three phases, caused by the reaction of Y_2O_3 additive and Al_2O_3 on the surface of AlN, depends on the oxygen content in the starting AlN powder and the content of Y_2O_3 additive [14-16]. The AlN sample debinded in air showed only $Y_3Al_5O_{12}$ secondary phase without Y_2O_3, in contrast with the AlN sample debinded in the N_2 atmosphere. This
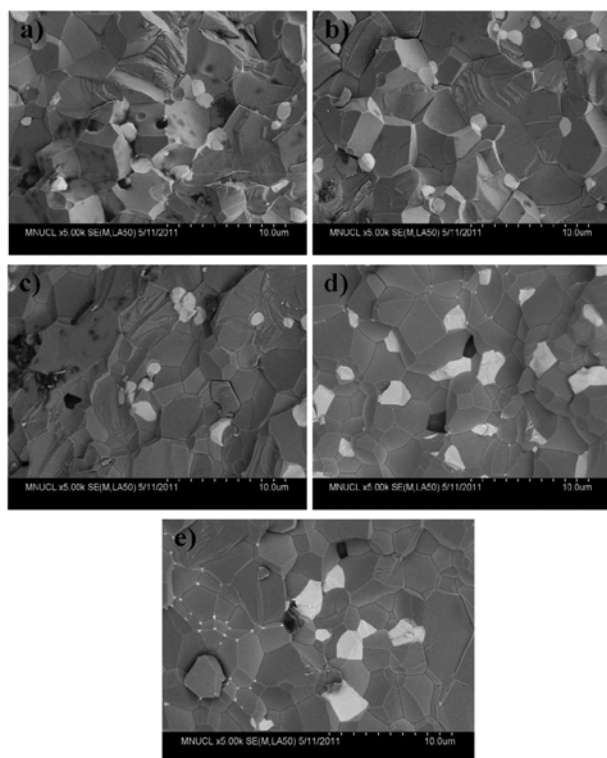
Fig. 5. The microstructures of sintered AlN samples ; a) sample #1, b) sample #2, c) sample #3, d) sample #4 and e) sample #5.
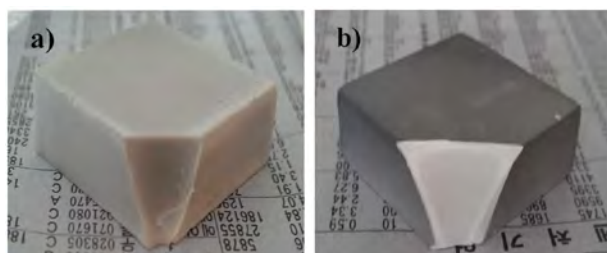

Fig. 6. Color of sintered AlN samples according to debinding condition : a) air atmosphere and b) N_2 atmosphere.

indicates that a greater amount of Al_2O_3 was formed on the surface of AlN powder debinded in air, and this resulted in the absence of Y_2O_3 for the formation of $Y_3Al_5O_{12}$ and decreased relative density and thermal conductivity, as shown in Fig. 3.

SEM micrographs of the sintered AlN specimens at each debinding atmosphere are presented in Fig. 5. The second-phase particles in the samples debinded in the air atmosphere were widely distributed and showed smaller grain size. In comparison, the second-phase particles in the samples debinded in the N_2 atmosphere were more concentrated on triple points and were larger. In general, the intergranular phase decreased during the isothermal hold time by the migration of a liquid phase consisting of Y_2O_3, Al_2O_3, and AlN. Comparison of the microstructures of AlN ceramics prepared with different amounts of Y_2O_3 additive and isothermal hold times revealed that with lower quantity

of intergranular phase, accordingly higher thermal conductivity is attained [17]. In this study, the formation of Al_2O_3 on the surface of the AlN powder debinded in the air atmosphere resulted in a wide distribution of the $Y_3Al_5O_{12}$ phase. Thus, the lower thermal conductivity of the AlN samples debinded in the air atmosphere may be related to the second-phase distribution [18]. On the other hand, it is speculated that, when the PVB binder was burned out in the N_2 atmosphere, some residual carbon played a role in decreasing the oxygen content in the AlN lattice, which resulted in higher thermal conductivity [19]. The sintered AlN samples showed different colors according to the debinding atmosphere. The color of the samples is presented in Fig. 6. The sample debinded in the N_2 atmosphere showed black (surface) and gray (inside) color, in contrast with the single color of the sample debinded in the air atmosphere. The different color may be caused by residual carbon. The sintered AlN prepared from the commercial powders showed similar results in terms of the final phase, microstructure, and sample color according to the debinding atmosphere.

Conclusions

The effects of the debinding condition on the final phase, microstructure and thermal conductivity of spray dried AlN powder compacts were investigated. $Y_3Al_5O_{12}$ secondary phase was observed with a wide distribution in the microstructure of the sintered AlN sample debinded in an air atmosphere and the sample showed lower thermal conductivity. These results are attributed to the formation of Al_2O_3 on the surface of the AlN powder due to the oxidizing atmosphere. In the sintered AlN sample debinded in a N_2 atmosphere, the color of the sample surface and interior was different due to the residual carbon, and the measured thermal conductivity was higher than that of the AlN debinded in the air atmosphere. The higher thermal conductivity was caused by the YAG phases being more concentrated on the triple points, and the residual carbon led to a decrease of oxygen content in the AlN lattice.

Acknowledgment

References

1. G.A. Slack, J. Phys. Chem. Solids 34 (1973) 321-335.
2. N. Iwamoto, in "Transactions of the Materials Research

Society of Japan, Vol. 3" The Materials Research Society of Japan (1992) 80.

3. Y. Baik and R.A.L. Drew, Key Eng. Mater. 122-124 (1996) 555-570.

4. I. Haase and G. Himple, Silicates Ind. 7-8 (1993) 143-148.

5. G.A. Slack, R.A. Tanzilli, R.O. Pohl, and J.W. Vandersande, J. Phys. Chem. Solids 48 (1987) 641-647.

6. K. Shinozaki and A. Tsuge, Bull. Ceram. Soc. Jpn. 21 (1986) 1130-1135.

7. T.B. Jackson, A.V. Virkar, K.L. More, R.B. Dinwideie, and R.A. Culter, J. Am. Ceram. Soc. 80 (1997) 1421-1435.

8. R. Lee, J. Am. Ceram. Soc. 74 (1991) 2242-2249.

9. Y.N. Sun, M.D. Sacks, and J.W. Williams, in "Ceramic Transactions, Vol. 1" The American Ceramic Society (1988) 538.

10. S.F. Horvath, S.R. Witek, and M.P. Harmer, in "Advances in Ceramics, Vol. 26" (The American Ceramic Society, 1989) 121.

11. K. Komeya, H. Inoue, and A. Tsuge, J. Am. Ceram. Soc. 57 (1974) 411.

12. L. Qiao, H. Zhou, H. Xue, and S. Wang, J. Euro. Ceram. Soc. 23 (2003) 61-67.

13. P.H. Klein and W.J. Croft, J. Appl. Phys. 38 (1967) 1063-1064.

14. J.C. Huseby and C.J. Bobik, U.S. Pat. No. 4578 365, (1986).

15. K. Schwetz, W. Grellneret, K. Hunold, M. Mohr, and A. Lipp, U. S. Pat. No. 4803 183 (1989).

16. K. Komeya, H. Inoue and A. Tsuge, Yogyo Kyokaishi 93 (1985) 41-47.

17. H. Nakano, K. Watari and K. Urabe, J. Euro. Ceram. Soc. 23 (2003) 1761-1768.

18. H. Yan, W.R. Cannon and D.J. Shanefield, J. Am. Ceram. Soc. 76 (1993) 166-172.

19. Y.D. Yu, A.M. Hundere, R. Hoier, R.E.D. Borkowski and M.A. Einarsrud, J. Euro. Ceram. Soc. 22 (2002) 247-252.